FINITE ELEMENT METHODS: 1970's AND BEYOND
L.P. Franca (Ed.)

THE STABILIZED FINITE ELEMENT METHOD FOR COMPRESSIBLE NAVIER STOKES SIMULATIONS : REVIEW AND APPLICATION TO AIRCRAFT DESIGN

Frederic Chalot
Dassault Aviation
78 quai Dassault
92214 Saint Cloud, France
Email: frederic.chalot@dassault-aviation.fr
Web page: http://www.dassault-aviation.com

Michel Mallet
Dassault Aviation
78 quai Dassault
92214 Saint Cloud, France
Email: michel.mallet@dassault-aviation.fr

Abstract. The solution of the compressible Navier Stokes equations constitutes a very challenging problem for applied mathematics. The methods developed using a finite element approach and Galerkin least - squares stabilized formulation will be reviewed. Various applications will be described to illustrate the capability of the method for aircraft design including space plane projects and long range business jets. Finally, general trends for future developments will be identified.

Key words: Navier - Stokes, compressible, entropy variables, finite element, stabilization, aerodynamics, aircraft design

1 INTRODUCTION

Solution of the compressible Navier Stokes equations presents many challenges for numerical analysis. One challenge is associated to the mixed hyperbolic / elliptic nature of the equations with different behavior for subsonic and supersonic flows; the equations include very strong non linearities and lead to solutions where discontinuities (shocks) can develop; solutions are mostly advection dominated but viscous contributions can go from a 10^{-6} perturbation to a dominant term; solutions also exhibit very anisotropic behavior due to boundary layers which impose space discretization with extremely high aspect ratios elements. Stabilized methods have demonstrated that they can offer very satisfactory answers to all those challenges.

Most initial efforts to develop methods for compressible flows relied on finite difference or finite volume approaches and often used Riemann solvers. T.J.R Hughes's group was among the few research groups which chose to follow a finite element strategy. An incomplete and very simplified listing of the successive steps in the development of stabilized methods for the compressible Navier Stokes equations within this group follows. It starts with a first extension of the original Brooks and

Hughes[1] scheme to the Euler equations.[2] Entropy variables,[3] the generalized SUPG operator[4] and discontinuity capturing operator[5] were proposed next. Theoretical analysis,[6] efficient implicit[7] and parallel[8] methods were then established. The next step was to extend the approach to complex thermodynamics.[9] The CFD group at Dassault has close links with these developments and progressively, at Dassault, varied and complex aircraft design applications have been performed.

The compressible Navier Stokes equations and the rational for using entropy variables will be presented in the first paragraph. The stabilized finite element method will be described next. In the last paragraph, a number of representative computations for aircraft design will be reviewed.

2 THE COMPRESSIBLE NAVIER STOKES EQUATIONS AND ENTROPY VARIABLES

As a starting point, we consider the Euler and Navier-Stokes equations written in conservative form:

$$\boldsymbol{U}_{,t} + \boldsymbol{F}_{i,i}^{\mathrm{adv}} = \boldsymbol{F}_{i,i}^{\mathrm{diff}} \tag{1}$$

where $\boldsymbol{U}$ is the vector of conservative variables : $\boldsymbol{U} = (\rho, \rho u, \rho v, \rho w, \rho e)$; $\boldsymbol{F}_i^{\mathrm{adv}}$ and $\boldsymbol{F}_i^{\mathrm{diff}}$ are, respectively, the advective and the diffusive fluxes in the i^{th}-direction. Inferior commas denote partial differentiation and repeated indices indicate summation.

Equation (1) can be rewritten in quasi-linear form:

$$\boldsymbol{U}_{,t} + \boldsymbol{A}_i \boldsymbol{U}_{,i} = (\boldsymbol{K}_{ij} \boldsymbol{U}_{,j})_{,i} \tag{2}$$

where $\boldsymbol{A}_i = \boldsymbol{F}_{i,\boldsymbol{U}}^{\mathrm{adv}}$ is the i^{th} advective Jacobian matrix, and $\boldsymbol{K} = [\boldsymbol{K}_{ij}]$ is the diffusivity matrix, defined by $\boldsymbol{F}_i^{\mathrm{diff}} = \boldsymbol{K}_{ij} \boldsymbol{U}_{,j}$. The $\boldsymbol{A}_i$'s and $\boldsymbol{K}$ do not possess any particular property of symmetry or positiveness.

We now introduce a new set of variables,

$$\boldsymbol{V}^T = \frac{\partial \mathcal{H}}{\partial \boldsymbol{U}} \tag{3}$$

where $\mathcal{H}$ is the generalized entropy function given by

$$\mathcal{H} = \mathcal{H}(\boldsymbol{U}) = -\rho s \tag{4}$$

and s is the thermodynamic entropy per unit mass. Under the change of variables $\boldsymbol{U} \mapsto \boldsymbol{V}$, (2) becomes:

$$\widetilde{\boldsymbol{A}}_0 \boldsymbol{V}_{,t} + \widetilde{\boldsymbol{A}}_i \boldsymbol{V}_{,i} = (\widetilde{\boldsymbol{K}}_{ij} \boldsymbol{V}_{,j})_{,i} \tag{5}$$

where

$$\widetilde{\boldsymbol{A}}_0 = \boldsymbol{U}_{,\boldsymbol{V}} \tag{6}$$

$$\widetilde{\boldsymbol{A}}_i = \boldsymbol{A}_i \widetilde{\boldsymbol{A}}_0 \tag{7}$$

$$\widetilde{\boldsymbol{K}}_{ij} = \boldsymbol{K}_{ij} \widetilde{\boldsymbol{A}}_0 . \tag{8}$$

The Riemannian metric tensor $\widetilde{\boldsymbol{A}}_0$ is symmetric positive-definite; the $\widetilde{\boldsymbol{A}}_i$'s are symmetric; and $\widetilde{\boldsymbol{K}} = [\widetilde{\boldsymbol{K}}_{ij}]$ is symmetric positive-semidefinite. (In view of these properties, (5) is referred to as a symmetric advective-diffusive system).

For dvantages of this change of variables are numerous: it provides strong mathematical and numerical coherence (dimensionally correct dot product, symmetric operators with positivity properties, efficient preconditioning). In addition, entropy variables yield further improvements over the usual conservation variables, in particular in the context of chemically reacting flows.[10]

a general divariant gas, the vector of so-called (physical) entropy variables, $\boldsymbol{V}$, reads

$$\boldsymbol{V} = \frac{1}{T} \begin{Bmatrix} \mu - |\boldsymbol{u}|^2/2 \\ \boldsymbol{u} \\ -1 \end{Bmatrix}$$

where $\mu = e + pv - Ts$ is the chemical potential per unit mass; $v = 1/\rho$ is the specific volume.

Taking the dot product of (5) with the vector $\boldsymbol{V}$ yields the Clausius-Duhem inequality, which constitutes the basic nonlinear stability condition for the solutions of (5). This fundamental property is inherited by appropriately defined finite element methods, such as the one described in the next section.

3 THE GALERKIN/LEAST-SQUARES FORMULATION FOR COMPRESSIBLE FLOWS

The Galerkin/least-squares (GLS) formulation is a full space-time finite element technique employing the discontinuous Galerkin method in time.[11] The least-squares operator ensures good stability characteristics while retaining a high level of accuracy. The local control of the solution in the vicinity of sharp gradients is further enhanced by the use of a nonlinear discontinuity-capturing operator.

We consider the time interval $I =]0, T[$, which we subdivide into N intervals $I_n =]t_n, t_{n+1}[$, $n = 0, \ldots, N-1$. Let

$$Q_n = \Omega \times I_n, P_n = \Gamma \times I_n \tag{9}$$

where Ω is the spatial domain of interest, and Γ is its boundary. In turn, the space-time "slab" Q_n is tiled by $(n_{\mathrm{el}})_n$ elements Q_n^e. Consequently, the Galerkin/least-squares variational problem can be stated as :

Within each Q_n, $n = 0, \ldots, N-1$, find $\boldsymbol{V}^h \in \mathcal{S}_n^h$ (trial function space), such that for all $\boldsymbol{W}^h \in \mathcal{V}_n^h$ (weighting function space), the following equation holds:

$$\int_{Q_n} \Big(- \boldsymbol{W}_{,t}^h \cdot \boldsymbol{U}(\boldsymbol{V}^h) - \boldsymbol{W}_{,i}^h \cdot \boldsymbol{F}_i^{\mathrm{adv}}(\boldsymbol{V}^h) + \boldsymbol{W}_{,i}^h \cdot \widetilde{\boldsymbol{K}}_{ij} \boldsymbol{V}_{,j}^h \Big) \, dQ$$

$$\int_{\Omega} \Big(\boldsymbol{W}^h(t_{n+1}^-) \cdot \boldsymbol{U}(\boldsymbol{V}^h(t_{n+1}^-)) - \boldsymbol{W}^h(t_n^+) \cdot \boldsymbol{U}(\boldsymbol{V}^h(t_n^-)) \Big) \, d\Omega$$

$$+\sum_{e=1}^{(n_{\rm el})_n}\int_{Q_n^e}\int_{Q_n^e}\Big(\mathcal{L}\boldsymbol{W}^h\Big)\cdot\boldsymbol{\tau}\Big(\mathcal{L}\boldsymbol{V}^h\Big)\,dQ+\sum_{e=1}^{(n_{\rm el})_n}\int_{Q_n^e}\nu^h g^{ij}\boldsymbol{W}^h_{,i}\cdot\widetilde{\boldsymbol{A}}_0\boldsymbol{V}^h_{,j}\,dQ$$
$$=\int_{P_n}\boldsymbol{W}^h\cdot\Big(-\boldsymbol{F}_i^{\rm adv}(\boldsymbol{V}^h)+\boldsymbol{F}_i^{\rm diff}(\boldsymbol{V}^h)\Big)n_i\,dP. \qquad (10)$$

The first and last integrals represent the Galerkin formulation written in integrated-by-parts form. The solution space consists of piecewise polynomials which are continuous in space, but are discontinuous across time slabs. Continuity in time is weakly enforced by the second integral in (10), which contributes to the jump condition between two contiguous slabs, with

$$\boldsymbol{Z}^h(t_n^{\pm})=\lim_{\varepsilon\to 0^{\pm}}\boldsymbol{Z}^h(t_n+\varepsilon).$$

The third integral constitutes the least-squares operator where $\mathcal{L}$ is defined as

$$\mathcal{L}=\widetilde{\boldsymbol{A}}_0\frac{\partial}{\partial t}+\widetilde{\boldsymbol{A}}_i\frac{\partial}{\partial x_i}-\frac{\partial}{\partial x_i}(\widetilde{\boldsymbol{K}}_{ij}\frac{\partial}{\partial x_j}). \qquad (11)$$

$\boldsymbol{\tau}$ is a symmetric matrix for which definitions can be found in.[11] The fourth integral is the nonlinear discontinuity-capturing operator, which is designed to control oscillations about discontinuities, without upsetting higher-order accuracy in smooth regions. g^{ij} is the contravariant metric tensor defined by

$$[g^{ij}]=[\boldsymbol{\xi}_{,i}\cdot\boldsymbol{\xi}_{,j}]^{-1} \qquad (12)$$

where $\boldsymbol{\xi}=\boldsymbol{\xi}(\boldsymbol{x})$ is the inverse isoparametric element mapping, and ν^h is a scalar-valued homogeneous function of the residual $\mathcal{L}\boldsymbol{V}^h$. The discontinuity capturing factor ν^h used in the present work is an extension of that introduced by Hughes, Mallet, and Shakib.[11]

A key ingredient to the formulation is its consistency: the exact solution of (1) satisfies the variational formulation (10). This constitutes an essential property in order to attain higher-order spatial convergence.

Convergence to steady state of the compressible Navier Stokes equations is achieved through a fully-implicit iterative time-marching procedure based on the GMRES algorithm.[7]

A low-storage extension based solely on residual evaluations was developed by Johan.[8] It reveals particularly adapted to parallel processing,[12] where the linear solver often constitutes a painful bottleneck.

4 APPLICATIONS

4.1 Design of the HERMES space plane

The first application of the NS code based on the Galerkin least squares approach was the aerothermal design of the Hermes space plane in the early 90's. This is illustrated by the calculation of the flow over the canopy of Hermes. It was performed at the most critical point on the reentry flight path for the windshield design: the

altitude is 60 km, the Mach number is 20 and the angle of attack is 30 degrees. At this altitude the Re/m is 120,890. The equilibrium real gas hypothesis was used along with radiative boundary conditions. The mesh includes approximately one million elements. The surface mesh is presented in Figure 1. The finite element approach allows mesh refinement and a precise representation of the details of the geometry in the windshield area. Considerable mesh density is used in the direction perpendicular to the wall. Stanton number isolines are presented in Figure 2. Complex flow structure is observed. Detailed discussion of Navier-Stokes calculations related to the aerothermal design of Hermes can be found in Naïm *et al*[13] and in.[14]

4.2 Design of the Crew Transfer Vehicle

Intensive parallel computing was used during the design process of a Crew Rescue/Crew Transfer Vehicle. Starting with the X-24, the final shape has been selected by NASA for its Crew Rescue Vehicle, and may as well serve as the basis for the future European Crew Transfer Vehicle. The transonic optimization of such a spacecraft required numerous detailed computations of the complex flow between the main body and the winglets. Thanks to the NEC SX-4 installed at NLR, key ingredients to the design, such as multi-point lift-versus-drag and pitching-moment-versus-angle-of-attack curves, could be computed overnight. Eight processors were used routinely on meshes made up of about 220,000 nodes for symmetric configurations. This design project was the first project to rely on the ability to perform a complete shape computation with overnight turn over. The reader is referred to[15] for further details about the design of the CRV/CTV.

For the purpose of illustration, we have selected an unsymmetrical configuration past one of the many spacecraft shapes which were considered in the design iteration process: the free-stream Mach number is 0.95, the angle of attack 20°, and the side-slip angle 5°. A view of the surface mesh is presented in Figure 5. The complete three-dimensional mesh contains about 500,000 nodes. Figure 6 shows the pressure-coefficient contours on the surface of the CRV/CTV; it gives an idea of the complex flow pattern which surrounds the vehicle.

4.3 Flow over a delta wing at high angle of attack

The flow over a delta wing at high angle of attack is characterized by a complex vortex structure and possible vortex breakdown. Accurate prediction of wing lift requires a good prediction of these vortices since the high velocity associated with the leeward vortices is associated with low pressure, while vortex breakdown will lead to a loss of lift. Fig 6 presents the vortex structure over a military wing at Mach 0.2 and an angle of attack of 25 degrees. A blunt generic forebody is included to avoid possibly unsteady cone vortices associated to a typical forebody. Slats are deflected at different angles. Three vortices are identified : one originating from the wing fuselage junction and two from each of the two slats. Computations have been performed with a two layer (k,eps) model and with an Explicit Algebraic Reynolds Stress model, the latter model yields improved results.

4.4 Afterbody of fighter aircraft

Computation of the flow over the afterbody of a military aircraft is performed with two objectives : to assess drag and to provide data for infrared stealth prediction. Afterbody flow includes many challenging features : normal shocks along the jet axis, compressible mixing layers with high density and temperature gradients, base flow and a possible shock wave - boundary layer interaction over the aft part of the fuselage. The thermodynamic model must account for the concentration and vibrational modes of species resulting from combustion that flow out of the nozzle. One example of such a computation is presented in Figure 6 for a two engine aircraft.

4.5 Transonic wing design

The design of a highly optimized wing for a long range jet flying at high transonic speed is one of the most complex task for aerodynamicists. Recent design computations using the Galerkin least squares approach is illustrated in Figure 7 where computed pressures are compared to wind tunnel results. Very good agreement is observed. Pressure sensitive paint is used in the wind tunnel to measure the pressure distribution over almost the entire wing. The computation accounts for the wind tunnel model static deformation under aerodynamic loads. Real wing deformation will be different since the structure of the wind tunnel model is not representative of the actual structure. A few hundred such computations have been performed over the duration of the design project. Several points over the polar curve are computed for each shape, several cruise Mach numbers are also considered. Buffet onset is predicted (buffet is an unsteady phenomena associated to shock wave - boundary layer interaction). A typical mesh includes about 1.5 millions nodes. A two layer (k,eps) model is used with non equilibrium corrections and a calibrated set of constants.

5 CONCLUSIONS

The main features of the Galerkin least squares method for compressible Navier Stokes simulations have been described. Important applications have been reviewed and illustrate the considerable progress made over the past 20 years and its impact on real life design. The next two decades should also seek to achieve ambitious goals. Future needs include accurate prediction of always more complex turbulent flows. This includes flows with complex interactions or large scale unsteady behavior and will require improved turbulence models. Large eddy simulation is a very promising approach[16] in particular in the framework of the variational multiscale method.[17] Its application to design will require further development, a zonal approach with coupling to RANS model might be needed for many applications. Automatic shape optimization has made considerable progress recently.[18] Its widespread application to various design problems still requires continued effort, in particular when viscous flow models are needed. Various multidisciplinary problems are already addressed using complex simulation sequences.[19] Examples include prediction of structural vibration (most notably flutter and buffet induced acceleration), the evaluation of infrared signature or airframe acoustic modeling. Future simulations will include further multidisciplinary problems with strong coupling between models.

ACKNOWLEDGEMENTS

The techniques and results presented in this paper have been obtained with contributions from many friends and colleagues both at Stanford and at Dassault, we would like to mention A. Davroux, L. Franca, J.M. Hasholder, K. Jansen, Z. Johan, A. Naim, M. Ravachol, J.P. Rosenblum, Ph. Rostand, F. Shakib, B.Stoufflet.

REFERENCES

[1] T.J.R. Hughes and A. Brooks, "A multidimensional Upwind Scheme with no Crosswind Diffusion", *Finite Element Methods for Convection Dominated Flows*, ASME, New York, 19-35 (1979).

[2] T.J.R. Hughes and T.E. Tezduyar, Finite element methods for first order hyperbolic systems with particular emphasis on the compressible Euler equations. North-Holland, *Computer Methods in Applied Mechanics and Engineering*, 45, 217-284 (1984).

[3] T.J.R. Hughes, L.P. Franca and M. Mallet, A new finite element formulation for computational fluid dynamics: I Symmetric forms of the compressible Euler and Navier Stokes equations and the second law of thermodynamics. North-Holland, *Computer Methods in Applied Mechanics and Engineering*, 54, 223-234 (1986).

[4] T.J.R. Hughes and M. Mallet, A new finite element formulation for computational fluid dynamics: III The generalized streamline operator for multidimensional advective - diffusive systems. North-Holland, *Computer Methods in Applied Mechanics and Engineering*, 58, 305-328 (1986).

[5] T.J.R. Hughes and M. Mallet, A new finite element formulation for computational fluid dynamics: IV A discontinuity-capturing operator for multidimensional advective - diffusive systems. North-Holland, *Computer Methods in Applied Mechanics and Engineering*, 58, 329-336 (1986).

[6] T.J.R Hughes, L.P. Franca and M. Mallet A new finite element formulation for computational fluid dynamics: VI Convergence analysis of the generalized SUPG formulation for linear time-dependent multidimensional advective diffusive system. North-Holland, *Computer Methods in Applied Mechanics and Engineering*, 63, 97-112 (1987).

[7] F. Shakib, T.J.R. Hughes, and Z. Johan, A multi-element group preconditioned GMRES algorithm for nonsymmetric systems arising in finite element analysis, *Computer Methods in Applied Mechanics and Engineering*, Vol. 75, pp 415–456, (1989).

[8] Z. Johan, T.J.R. Hughes, and F. Shakib, A globally convergent matrix-free algorithm for implicit time-marching schemes arising in finite element analysis in fluids, *Computer Methods in Applied Mechanics and Engineering*, Vol. 87, 281–304, (1991).

[9] F. Chalot, T.J.R. Hughes, and F. Shakib, "Symmetrization of conservation laws with entropy for high-temperature hypersonic computations," *Computing Systems in Engineering*, 1, 465–521 (1990).

[10] F. Chalot, M. Mallet, and M. Ravachol, A comprehensive finite element Navier-Stokes solver for low- and high-speed aircraft design, paper #94-0814, *AIAA 32nd Aerospace Sciences Meeting*, Reno, NV, January 10–13, (1994).

[11] F. Shakib, T.J.R. Hughes, and Z. Johan, A new finite element formulation for computational fluid dynamics: X. The compressible Euler and Navier-Stokes equations, *Computer Methods in Applied Mechanics and Engineering*, Vol. 89, pp 141–219, (1991)

[12] F. Chalot, Q.-V. Dinh, M. Mallet, A. Naïm, and M. Ravachol, "A Multi-platform Shared- or Distributed-Memory Navier-Stokes Code," *9th International Conference on Parallel CFD*, Manchester, UK, May 19–21, (1997).

[13] A. Naïm, M. Mallet, Ph. Rostand, and J.M. Hasholder, "Local aerothermal problems during Hermes reentry," *Theoretical and Experimental Methods in Hypersonic Flows*, AGARD Conference Proceedings 514, pp. 42-1–42-16, (1993).

[14] R. Hagmeijer, B. Oskam, K.M.J de Cock, P. Perrier, Ph. Rostand, J.M. Hasholder, and J.W. Wegereef, "Validation of the design of the computational methods used for the design of the canopy of the Hermes spaceplane," paper #94-1865, *AIAA 12th Applied Aerodynamics Conference*, Colorado Springs, CO, June 20–22, (1994).

[15] F. Chalot, J.M. Hasholder, M. Mallet, A. Naïm, P. Perrier, M. Ravachol, Ph. Rostand, B. Stoufflet, B. Oskam, R. Hagmeijer, and K. de Cock, "Ground to flight transposition of the transonic characteristics of a proposed Crew Rescue/Crew TransferVehicle," paper #97-2305, *15th AIAA Applied Aerodynamics Conference*, Atlanta, GA,June 23–25, (1997).

[16] F. Chalot, B. Marquez, M. Ravachol, F.Ducros, F. Nicoud, Th. Poinsot, "A consistent Finite Element Approach to Large Eddy Simulation," paper #98-2652, *29th AIAA RFluid Dynamics Conference*, Albuquerque, NM, June 15-18, (1998).

[17] T.J.R. Hughes, L. Mazzei, K. Jansen, Large Eddy Simulation and the variational multiscale method, *Computing and Visualization in Science*, 3:47-59, (2000).

[18] Q.V. Dinh, S. Kleinveld, P. Ribaute, G. Roge, CFD-based aerodynamic shape optimization, Proceedings of the CEAS conference, Koln, June 25-27, (2001).

[19] F. Chalot, T. Fanion, M. Mallet, M. Ravachol and G. Roge, "Status and future challenges of CFD in a coupled simulation environment for aircraft design", Coupling of Fluids, Structures and Waves in Aeronautics , *Notes on Numerical Fluid Mechanics and Multidisciplinary design - Volume 85*, Springer, 277-286 (2003).

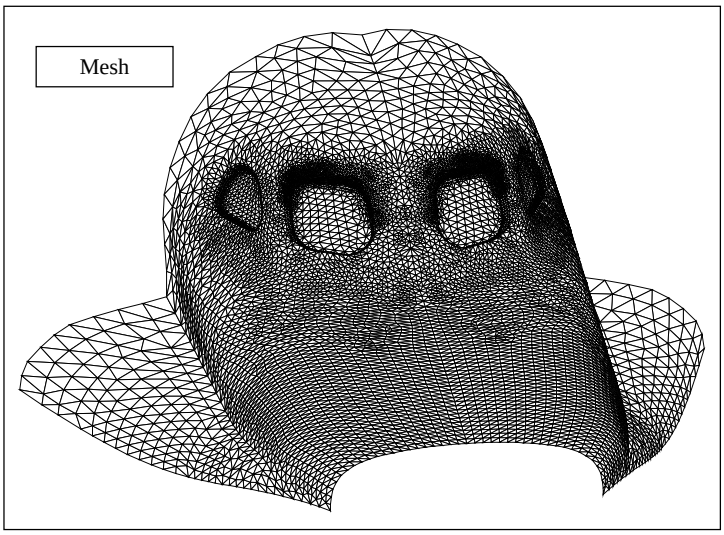

Figure 1: HERMES wind shield - surface mesh

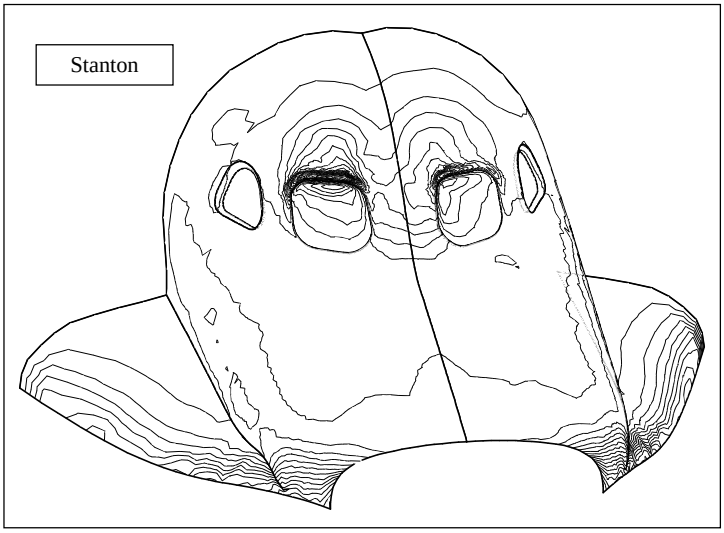

Figure 2: HERMES wind shield - surface heat flux

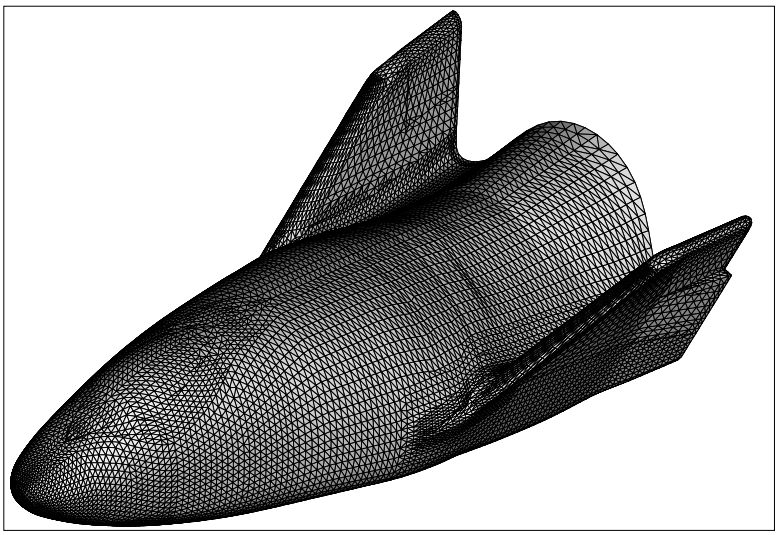

Figure 3: Crew transfer vehicle - surface mesh

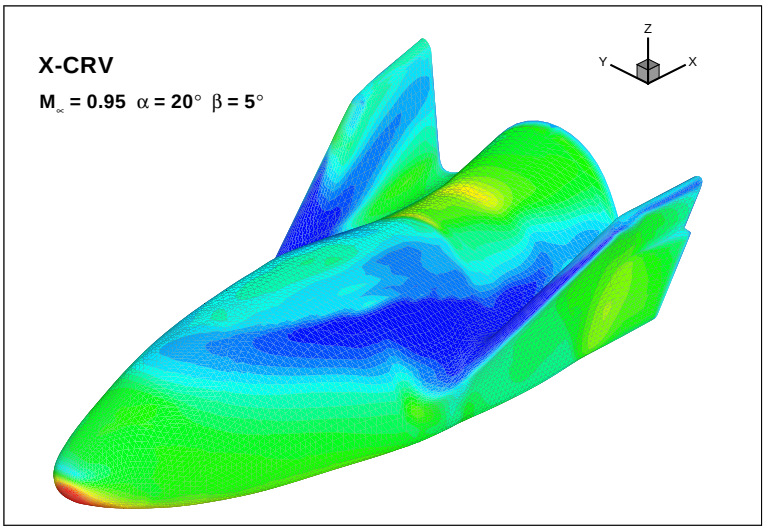

Figure 4: Crew transfer vehicle - surface pressure

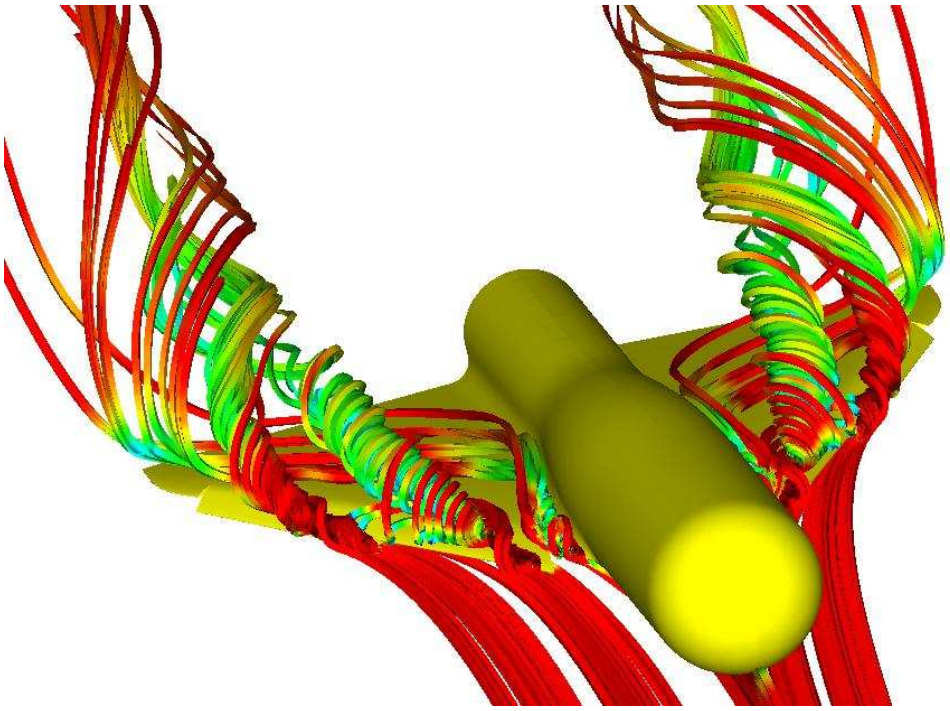

Figure 5: Flow over a delta wing with slats

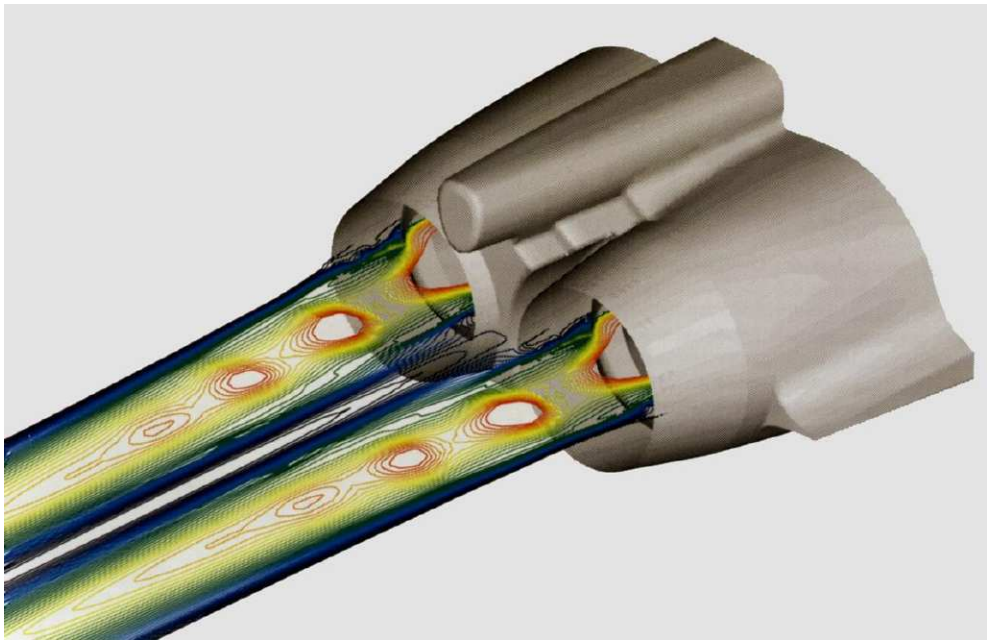

Figure 6: Afterbody flow

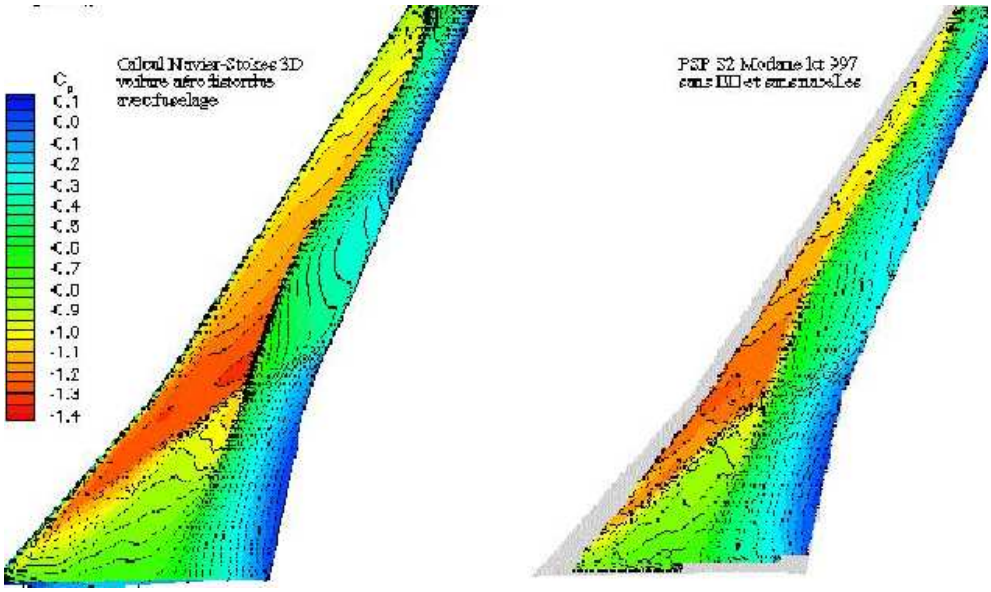

Figure 7: Transonic wing